THE JOURNAL OF PHYSICAL CHEMISTRY C

Article

Gold Dispersion and Activation on the Basal Plane of Single-Layer MoS

Cindy S. Merida, Duy Le, Elena M. Echeverría, Ariana E. Nguyen, Takat B Rawal, Sahar Naghibi Alvillar, Viktor Kandyba, Abdullah Al-Mahboob, Yaroslav B. Losovyj, Khabiboulakh Katsiev, Michael D. Valentin, Chun-Yu Huang, Michael J. Gomez, I-Hsi Lu, Alison Guan, Alexei Barinov, Talat S Rahman, Peter A. Dowben, and Ludwig Bartels

J. Phys. Chem. C, **Just Accepted Manuscript** • DOI: 10.1021/acs.jpcc.7b07632 • Publication Date (Web): 09 Dec 2017

Gold Dispersion and Activation on the Basal Plane of Single-Layer MoS_2

Cindy S. Merida,[1] Duy Le,[2] Elena M. Echeverria,[3] Ariana E. Nguyen,[1] Takat B. Rawal,[2] Sahar Naghibi Alvillar,[1] Viktor Kandyba,[4] Abdullah Al-Mahboob,[4] Yaroslav Losovyj,[5] Khabiboulakh Katsiev,[6] Michael D. Valentin,[1] Chun-Yu Huang, [1] Michael J. Gomez, [1] I-Hsi Lu, [1] Alison Guan, [1] Alexei Barinov,[4] Talat S. Rahman,[2] Peter A. Dowben,[3] Ludwig Bartels[1,*]

[1] *Department of Chemistry and Materials Science & Engineering Program, University of California - Riverside, Riverside, CA 92521, U.S.A.*

[2] *Department of Physics, University of Central Florida, 4000 Central Florida Blvd., Orlando, FL 32816, U.S.A.*

[3] *Department of Physics and Astronomy, Theodore Jorgensen Hall, 855 N 16th, University of Nebraska, Lincoln, NE 68588-0299, U.S.A.*

[4] *Elettra-Sincrotrone Trieste, S.S.14, 163.5 km, Basovizza, Trieste, Italy*

[5] *Department of Chemistry, Indiana University, 800 E. Kirkwood Ave. Bloomington, IN 47405, U.S.A.*

[6] *4700 King Abdullah University of Science and Technology, 2462 Thuwal 23955-6900, Kingdom of Saudi Arabia*

Corresponding Author Email: bartels@ucr.edu

Abstract

Gold islands are typically associated with high binding affinity to adsorbates and catalytic activity. Here we present the growth of dispersed nanoscale gold islands on single layer MoS_2, prepared on an inert SiO_2/Si support by chemical vapor deposition (CVD). This study offers a combination of growth process development, optical characterization, photoelectron spectroscopy at sub-micron spatial resolution, and advanced density functional theory modeling for detailed insight into the electronic interaction between gold and single-layer MoS_2. In particular, we find the gold density of states in Au/MoS_2/SiO_2/Si to be far less well-defined than Au islands on other 2-dimensional materials such as graphene, for which we also provide data. We attribute this effect to the presence of heterogeneous Au adatom/MoS_2-support interactions within the nanometer-scale gold cluster. Theory predicts that CO will exhibit adsorption energies in excess of 1 eV at the Au cluster edges, where the local density of states is dominated by Au $5d_{z2}$ symmetry.

Introduction

Transition metal dichalcogenides (TMDs) such as MoS_2 have many and diverse technologically application ranging from chemical catalysis, to emerging microelectronic integration as well as lubrication of surfaces. In particular, MoS_2 is the key industrial catalyst for hydrodesulfurization of crude oil;[1] other catalytic applications of MoS_2 include the formation of alcohols from syngas,[2] as reverse water-gas shift catalyst,[3, 4] and for facilitation of the hydrogen evolution reaction in electrocatalysis.[4, 5] While oxide-based catalytic compounds are frequently enhanced by metal nanoparticles, MoS_2 single-layer islands support a metallic state at their edge to which catalytic properties have been attributed.[6] At the same time, gold nanoparticles have demonstrated catalytic properties[7-9] different from bulk gold that are substrate- and particle-size dependent. On the archetypical 2-dimensional van der Waals material, graphene, gold aggregates even at very low dosages forming a bulk-like electronic structure that is catalytically inactive.[10, 11] Substantial substrate interactions are required to prevent surface aggregation of this most noble of elements;[12] reducible oxide surfaces such as titania or ceria are typically used for gold dispersion.[13, 14]

Here we investigate the binding of gold to a single-layer MoS_2 films on an oxide support and explore the shape/electronic properties of the resulting gold overlay. The goal is to understand the gold-MoS_2 substrate interactions, followed by the electronic structure of the resulting nanocluster, and their catalytic activity as a function of size[15-17]. Gold nanoparticles have been investigated on MoS_2,[18] for instance for electrode applications[19] and as a target for optical control of particle properties.[20] We find that the MoS_2 van der Waals basal plane differs substantially from graphene: gold is dispersed into clusters small enough to exhibit an electronic structure typical of catalytically active gold including a shift/broadening of the d-band position.

Our findings confirm the computational predictions of Rawal et al. [21] that suggest Au nanoparticles to bind strongly to single-layer MoS_2; Rawal et al. [21] underscore the potential of the Au/MoS_2 materials system for catalytic application. Furthermore, unlike several prior studies that define the impact of the substrate on the catalytic activity as indirect, i.e. caused by preventing aggregation but not by specific chemical gold-substrate interactions,[22, 23] our computational studies trace the potential catalytic activity of the Au/MoS_2 system to the emergent electronic structure of the composite. We note that recent studies of Au on h-BN[24-26] also suggest substantial Au island to substrate interactions.

There is a resemblance between MoS_2 particles found in actual catalysts[27] and the single-layer islands we can prepare efficiently on an otherwise inert substrate. The availability of the latter on a flat substrate renders them better accessible to spatially and angular resolved photoelectron spectroscopy while not compromising the relevance of our results. We find that the MoS_2 layer acts as a facile gold-dispersion interlayer. In this regard, our approach offers a direct counterpoint to prior work by Besenbacher and Lauritsen's group, in which MoS_2 was prepared on bulk gold and its properties investigated.[6]

Single-layer MoS_2 can be grown by CVD on a broad range of substrates to coat them in a near-conformal fashion offering scalable access to the material system investigated here. MoS_2 single- (or few-)layer coating leading to Au-dispersion and -activation on a comparatively inert substrate like SiO_2, that otherwise does not general support gold dispersion, has potential appeal for extending the use of gold nanoparticle catalysts to a broader range of support materials with unique thermal, mechanical and porosity properties.

Single- and few-layer TMDs films have recently attracted intense interest for electronic applications as semiconducting 2D counterparts of graphene.[28, 29] A large number of

photoelectron spectroscopy studies have addressed in this context the band structure of MoS_2 both in the bulk and thinned (generally by mechanical exfoliation) to the single-layer limit.[30-33] These provide us with reference ascertaining that the CVD MoS_2 material employed in this study exhibits the anticipated band structure near Γ (see supporting information).[34, 35] Analysis of the Fermi level position of our material ascertains low sulfur vacancy defect density. We note that in prior studies we addressed the activation of MoS_2 by sulfur depletion[36, 37] – and do not see any such effects in this study.

This study combines chemical vapor deposition (CVD) growth of single-layer single-crystalline MoS_2 [34] on ultra-thin SiO_2 on Si substrates, high-resolution synchrotron-based spectro-imaging and ultraviolet photoelectron spectroscopy, and density functional theory (DFT) modeling to understand the binding of gold to the basal plane of single-layer MoS_2 as a function of gold coverage (Figure. 1a).

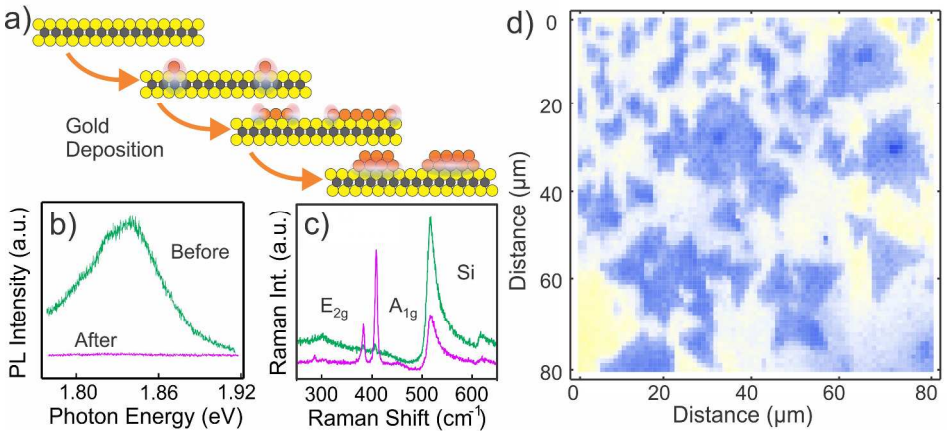

Figure 1 a) Schematic representation of the experiment and results: as the Au coverage on single-layer MoS_2 islands increases from isolated atoms to single- an bi-layer islands, strong Au-MoS_2 interaction at isolated atoms, island edges and the bottom layer modify the Au 5d density of states. The layer thickness/island density is for illustrative purpose and does not reflect the experimental values quantiatively; b) Photoluminescence (PL) spectroscopy shows bright signal at the optical bandgap of MoS_2 prior to gold deposition and complete quenching following deposition of 4Å of gold; c) Raman spectroscopy reveals surface enhanced MoS_2 E_{2g} and A_{1g} signal once the gold is deposited (at unchanged position) as well as attenuation of the Si substrate peak; d) map of the lateral variation of the photoelectron yield reveals the size and location of the single-layer single-crystalline MoS_2 islands used in this study.

Methods

Chemical Vapor Deposition Growth of MoS_2 Islands: This work employs chemical vapor deposition (CVD) molybdenum disulfide (MoS_2) single-layer single-crystalline islands grown onto a ≈1 nm SiO_2 film supported by a silicon wafer. CVD growth follows Ref. [34] and proceeded in a quartz tube furnace utilizing molybdenum trioxide (MoO_3, Aldrich) and elemental sulfur (Aldrich) as precursors. Inert nitrogen gas was used to transfer sulfur vapor from an alumina boat held slightly above the sulfur's melting temperature to the hot (650° C) reaction zone at the tube furnace center, where the target substrate was supported from a second alumina boat that also contained a small quantity (50 mg) of MoO_3. Single-layer MoS_2 island deposition and ripening occurred over 10 minutes at the maximum furnace temperature followed by a slow cool-down.

Optical Characterization of Single-Layer MoS_2 Material: Optical characterization utilizes a Horiba LabRAM system and a laser at a wavelength of 532 nm. Because of the absence of sizeable oxide layer, the single-layer MoS_2 islands are barely revealed in optical imaging. Photoluminescence and Raman spectroscopy utilizes an excitation power of 0.1 mW focused on a diffraction limited spot. The same sample area was investigated prior and after gold deposition.

Photoelectron Spectroscopy and Gold Deposition: The ARPES experiments were performed at the 3.2L spectromicroscopy undulator beamline of the Elettra light source at a temperature of 99 K using a photon energy of 27 eV. The incident radiation was linearly polarized (along the horizontal direction) and focused on a 0.6 μm diameter spot by means of a Schwarzschild objective[2]. An incident angle of 45° with respect to the sample surface was used to optimize

surface sensitivity. The ARPES data was acquired using a hemispherical electron energy analyzer with a combined energy resolution of 50 meV and angular resolution of <1°. The sample was mounted onto a scanning stage, which enabled positioning and raster imaging with respect to the fixed photon beam. Prior to photoelectron spectroscopy, the sample was annealed to 250°C to remove any spurious water adsorption. Gold deposition took place *in-situ* inside the same ultra-high vacuum system at a rate of 0.05 Å/s using a thermal evaporator and a quartz crystal microbalance for calibration.

Computational Approach: Our DFT simulations employ the projector-augmented wave (PAW)[38, 39] and plane wave basis set methods. We used the Perdew-Burke-Ernzerhof functional (PBE)[40] to describe the electronic exchange-correlation together with the DFT-D3 correction[41] for accounting wan der Waals interactions. The energy cutoff for plane-wave expansion was set at 500 eV, which is sufficient for energy and force convergences. The simulation supercell consists of an 8×8 single layer MoS_2 constructed using the optimized lattice parameter (a= 3.16 Å), an Au cluster adsorbed on one side of the MoS_2 layer and a vacuum of about 15 Å to separate the resultant structure with its normal periodical image. Because of the large supercell, we sample the Brillouin Zone with one point locating at the zone center for structural relaxation (with residual force of less than 0.01 eV/Å) and a 3×3×1 k-point mesh centered at the zone center for density of states (DOS) calculations. For visualization purpose, we use a Gaussian filter with $\sigma = 0.1$ eV to obtained DOS. Since the structures of the Au clusters are not resolved in experiment, and unknown, it is impossible to have one-to-one correspondence between experiment and simulation. Thus, for demonstration purpose, we choose Au clusters of 1, 7, 19, and 31 atoms, representing the smallest, two hexagonal-one-layer, and one hexagonal-bilayer clusters, respectively. For each cluster, we survey several adsorption configurations on MoS_2 and

we find that the lowest energy one is the one in which the center Au atom is on top of an S atom of MoS_2. The DOS analyzed and presented in this work are those of the lowest energy configurations.

Results

The material used in this study shows the expected bright photoluminescence (PL) and Raman features of single-layer MoS_2 (Figure1b,c).[28, 29, 34] The photoluminescence is slightly red-shifted as typically found in the absence of an SiO_2 buffer layer. The MoS_2 Raman features are less pronounced than on, for instance, SiO_2 due to substrate screening.[42] We observe the E_{2g} and A_{1g} modes are found at is 383 cm^{-1} and 408 cm^{-1}, respectively, and attribute the comparatively wide Raman mode separation to the same substrate interactions that cause strong substrate adhesion to bare Si. Notably, the small mode separation of single layer material is due to the absence of bonding to layers above and below. The case of an interacting substrate, like the silicon used in this study, differs from inert oxide typically used in studies of single-layer MoS_2. It is not astonishing that the out-of-plane vibrational A_{1g} mode is hardened in the presence of this interacting substrate, while the in-plane E_{2g} mode remains at the value expected for single-layer material.

We find significant enhancement of the MoS_2 Raman signal after deposition of 4 Å of gold indicative of the presence of very small gold islands that support plasmon-enhanced Raman measurements[43] or surface enhance Raman (SERS). Complete quenching of the PL signal after gold deposition at low average coverage indicates high dispersion of the gold (either as a continuous film or into small clusters) and absence of a combination of large-scale aggregation

and empty areas (which would retain their PL signal). We not that a layered (Frank van der Merve) growth of Au on MoS_2 can be ruled out given the high surface energy of gold and the comparatively low growth temperatures; thus, the efficient quenching of the MoS_2 PL signal observed in this study directly indicates the formation of highly-dispersed small-size gold aggregates.

Mapping of the photoelectron yield across the substrate reveals that the substrate is covered with an array of single-crystalline triangular MoS_2 islands of ≈10 micron in size interspersed between islands that originate from more than one nucleation spot and, consequently, contain a limited number of internal rotational domains (Figure 1d). Optical imaging of the islands on the substrate offers very low contrast because of the absence of a sufficient oxide layer underneath the single-layer MoS_2 islands.[44]

Figure 2a shows a series of photoelectron spectra taken at the same spot as the Raman and PL measurements of Figure. 1b,c on a single-layer MoS_2 islands (shown in Figure 1d) as the gold coverage was successively increased from 0 to 0.5, 1, 2 and 4 Å (approximately 0, 0.2, 0.4, 0.8, 1.6 monolayers, respectively). The final average coverage falls slightly short of a bilayer of gold. The angle-integrated spectra are based on angular-resolved measurements that at no and low gold coverage exhibit the known MoS_2 dispersion near the Γ point (see supporting information for energy-momentum diagrams). The supporting information section also includes a comparison of spectra taken at different islands to validate the reproducibility of the results and the homogeneity of the sample.

The spectra of Figure 2a show a prominent feature at ≈1.4 eV below E_F that shifts down slightly to higher binding energies as the gold coverage increases. We identify this photoemission feature as having significant MoS_2 valence band weight. Given a MoS_2 bandgap of 2.1-2.5 eV (roughly

equivalent to the optical bandgap of 1.87 eV plus exciton binding energy),[45-47] the position of the valence band edge at Γ (which is slightly below that at K) bespeaks a largely undoped material. This observation affirms the high quality of the CVD MoS_2 single-layer film of this study, because the typical defects in MoS_2 material, sulfur vacancies, act as n-type dopants. From the small value of the Fermi level shift ΔE_F away from the midgap position by only 0.1-0.3 eV and a straightforward application of the standard formula for the Fermi level shift $\Delta E_F = k_B T ln \frac{n_{doping}}{n_{intrinsic}}$ based on the Boltzmann constant (k_B), the temperature (T) and the defect-induced vs. intrinsic charge carrier concentration ($n_{doping}/n_{intrinsic}$), we obtain a value of the defect-induced free carrier concentration far smaller than one per square micron. While this analysis omits carriers trapped by chemical passivation of the vacancies, it clearly points to a defect density in our samples that is so low that defects will not determine the overall material properties.

The small down-shift (~200 meV) of the valence band edge with increased gold coverage suggests strong interactions between MoS_2 and the adlayer Au, and possibly very moderate additional *n*-type doping of the MoS_2 material as well. Analysis of the gold-induced Fermi-level shift (ΔE_F) in a similar fashion as described above suggests that it reflects transfer of only a fractional charge per few-micron island. While a precise numeric analysis of the MoS_2 valence band peak position is precluded by the non-trivial background, it is clear that the majority of the shift in our experiments occurs even before a monolayer of gold is reached, suggesting the significance and chemical strength of the direct interaction between the gold adatoms and the substrate. This interaction – and its catalytic implications – shall be the focus of the remainder of the manuscript.

Deposition of gold on single-layer MoS_2 leads to a broad density of states (DOS) contribution at 3-4 eV below the Fermi level. Comparing the electronic structure of low coverages of gold on MoS_2 to that of gold on graphene (Figure 2c), the absence of a well-defined and sharp gold 5d peak or doublet (dashed lines) is noticeable. Gold is known to aggregate into islands (Vollmer Weber Growth) on graphene and graphite, giving rise to extended gold aggregates of well-defined metallic band structure even at very low average coverage.[10, 11] In contrast, both the rapid attenuation of the MoS_2 valence band peak with gold deposition in the dataset of Figure 2a (a numerical analysis is shown in the supporting information) and the emergence of a broad gold 5d peak suggest the contrary for deposition onto MoS_2. In further support of this interpretation, we performed scanning tunneling microscopy imaging of comparable gold coverages on cleaved (bulk) MoS_2 surfaces and find the formation of highly-dispersed small islands.[48] Prior vibrational spectroscopy also suggests strong mechanical attachment in this material system.[49]

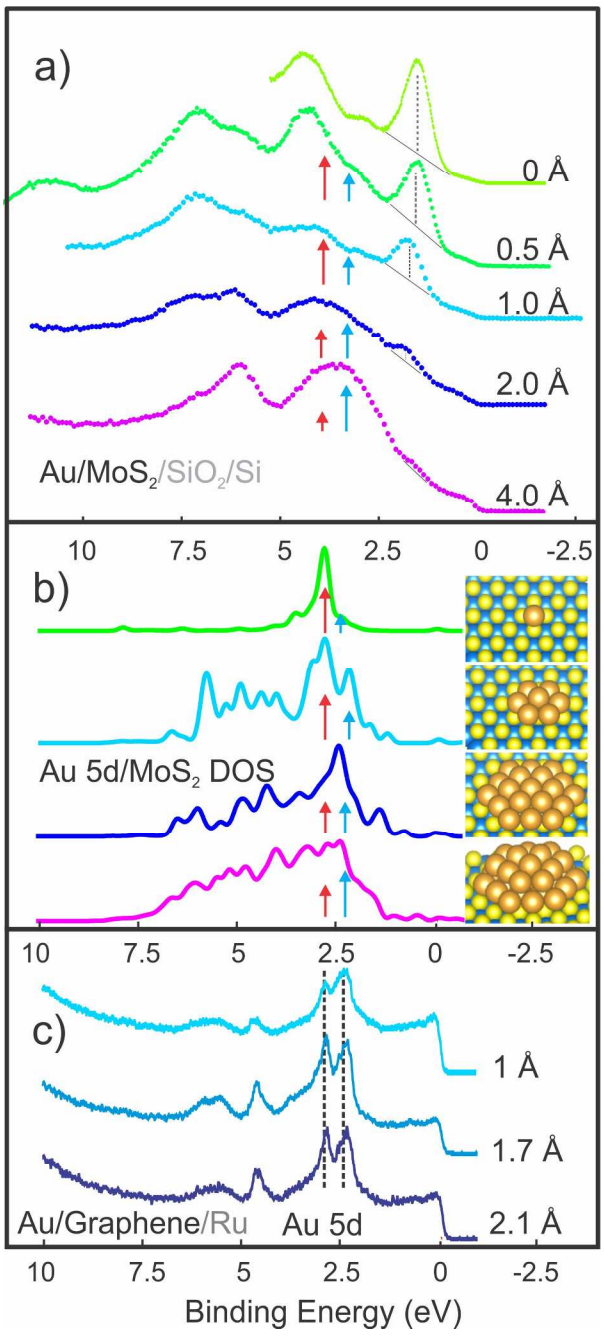

Figure 2 a) Experimental valence band spectra of Au on the same spot of an island of single-layer $MoS_2/SiO_2/Si$. With increasing gold coverage (~2.5Å correspond to a monolayer of gold), the Au-derived signal dominates the spectrum and shifts from higher (red arrow) to lower (blue arrow) binding energy while the MoS_2 VB intensity (dashed line) is reduced and broadened by Au-MoS_2 interactions; b) computational Au 5d density of state of the four clusters indicated. As the cluster size increases, lower binding energy gold DOS (blue arrow) augments and ultimately overshadowed the higher binding energy DOS (red arrow) found for a single Au atom. As these calculations do not include the SiO_2/Si substrate and any ensuing surface band bending, the Fermi level position (x-axis) was adjusted for optimal match with the experimental data; c) experimental reference spectra of Au on graphene show a clear Au 5d doublet and pronounced Fermi edge indicative of large metallic island formation and low substrate interaction, much in contrast to Au/MoS_2.

Discussion

DFT modeling of the total density of states of gold aggregates of different sizes and shapes on a single layer thick sheet of MoS_2 provides insight into the strength of the Au-MoS_2 interaction at the root of the high dispersion and absence of aggregation. Figure 2b shows the Au 5d DOS of an individual gold atom as well as two flat and one bilayer gold clusters on MoS_2. The calculations do not include the SiO_2/Si substrate and, hence, do not describe any substrate-effects on the Fermi level position. A single gold atom exhibits a prominent Au 5d-derived DOS contribution at a binding energy of ~2.5 eV (red arrow). As the size of the gold aggregate on MoS_2 increases, a number of additional 5d-derived DOS contributions emerge both at higher binding energy and at ~2.4 eV (blue arrow). The latter dwarves the former as the island size reaches 19 Au atoms (navy in Figure 2b). This trend can also be observed in the experimental data (Figure 2a), where a similar shift of peak intensity toward lower binding energy occurs as the Au coverage increases. Unfortunately, the multitude of substrate contributions prohibit numeric spectral deconvolution.

Our findings pose the question of the origin of aforementioned two spectral contributions – and how they emerge from Au-MoS_2 interactions. Figure 3 plots the spatial distribution of the dominant contribution to the local density of states (LDOS); volume elements, in which the LDOS at the higher binding energy dominates are colored in red, while volume elements in which the lower binding energy state dominates are colored in blue. The top panels show the LDOS distributions in the two energy intervals individually. In the case of the single atom, the higher binding energy state is in the surface plane whereas the, whereas the lower binding energy is of dz^2 (a_1) symmetry. The 19-atom cluster is held on the substrate by interactions at its edge

leading to a very moderate curvature in the cluster similar to that found in the top layer of the bilayer cluster.

Islands of different sizes share in common that at their perimeter or at their bottom (in the case of the bilayer island), i.e., wherever the interaction with the MoS_2 is enhanced, the higher binding energy state dominates, and elsewhere the lower binding energy one. The cross-sectional views affirm that the higher binding energy state hybridizes significantly with the top sulfur layer of the substrate, whereas the lower binding energy state does not.

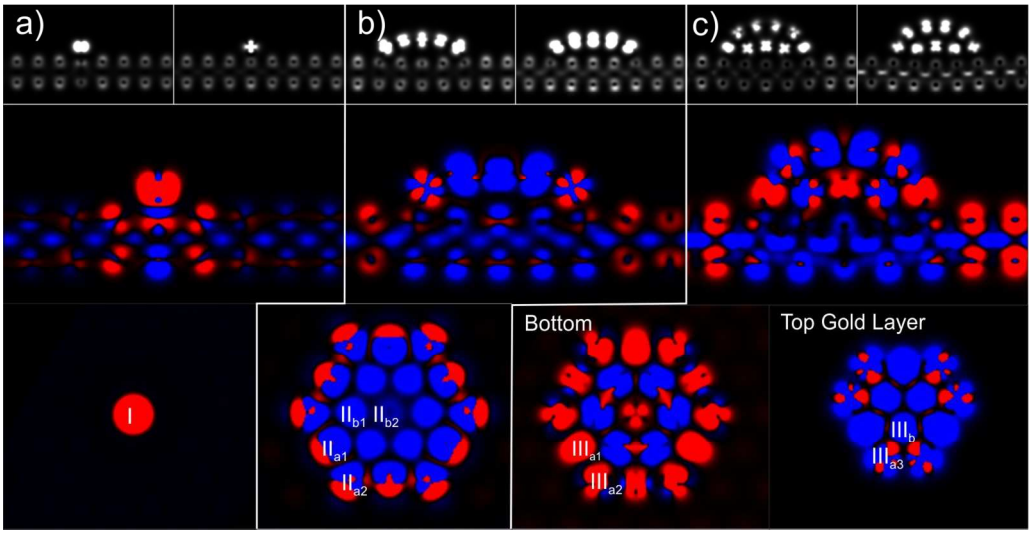

Figure 3 Comparison of the distribution of the density of state in the energy intervals marked by the red and blue arrows of Figure 2 (top row, left and right respective) and represented as difference for a) a single gold atom, b) a 19 atom cluster and, c) a bilayer 31 atom cluster of gold on MoS_2. The MoS_2-affected gold DOS is consistently found at the perimeter of the cluster suggesting propensity for activity of this particular region. Test sites for CO adsorption are labeled by roman numerals followed by *a* and *b* for a site at which the higher or lower binding energy state dominates, respectively.

The gold d-band position and its hybridization[21, 50] have been determined to be a crucial descriptor of its catalytic activity. Hence, the ability of single-layer MoS_2 to interact sufficiently strongly with gold to affect a major descriptor of its catalytic potential suggests that MoS_2 may have a use wherever a corresponding shift of the Au 5d state is desired.

Computationally the resultant affinity of the Au clusters to adsorption of CO molecules depends very much upon Au cluster size and the site. The various CO adsorption sites investigated are indicated in Figure 3 by Roman numerals standing for the cluster size followed by labels a,b to indicate whether the location is one at which the higher or lower binding energy LDOS dominates, respectively.

The results (Figure 4) exhibit significant variation of the CO adsorption energy between different CO adsorption sites ranging from practically no chemical bonding (~0.01 eV) in the center of the single-layer island (II_{b2}) to quite strong bonding (1.2 eV, about double that found on gold low-index surfaces) at the isolated gold atom and the perimeter sites of the clusters. The latter originates from a combination of enhanced CO-gold and CO-substrate interactions in binding configurations strongly tilted toward the surface plane. In each case, we find that the locations on the cluster, in which the Au-MoS_2 substrate interactions rendered the higher binding energy Au 5d component dominant, the CO binding energy exceeded that of the other sites and also that of bulk gold surfaces. On average, we find that the enhancement of the gold-CO interaction diminishes with increasing cluster size (dashed lines in Figure 4) toward the typical binding energy of CO on Au of 0.6 eV (0.42 eV in our calculations) observed both for the bulk and for gas-phase clusters of increasing size.[51] These results are also in agreement with the well-established inactivity of bulk gold and the findings of Ref. [21] for O_2 adsorbates.

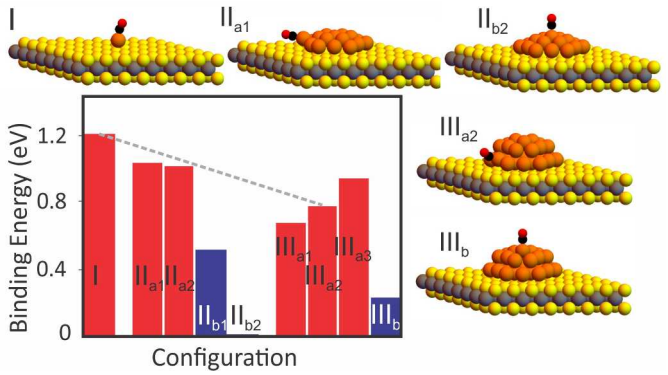

Figure 4 Impact of substrate interactions: the bar graph shows the adsorption energy of a CO molecule at different locations on a single Au atom (I), on a single-layer Au cluster (II), and on a bilayer Au cluster (III). Site labels are defined in Figure 3 and examples of the adsorption geometries are shown. The color coding of the bars represents the dominance of the higher/lower (red/blue) binding energy LDOS as shown in Figure3.

The computational approach also allows us to compare the binding energy of CO molecules on gold clusters supported by MoS_2 to CO binding to unsupported gold clusters of the same shape. We find that in the configurations these clusters are held in by MoS_2, they are also expected to exhibit strong binding in the gas phase. The supporting information provides a comparison.

Conclusion

Our combined experimental-computational investigation finds that single-layer MoS_2 islands can be prepared by scalable chemical vapor deposition techniques on a very thin oxide substrate where they offer an electronic structure closely resembling that of exfoliated MoS_2 and, most importantly, capable of interacting sufficiently with gold atoms so as to cause dispersion into small clusters. The resultant clusters are locked into a shape that is associated with undercoordination of edge gold atoms sustaining the substrate interaction and generating strong affinity for binding of small molecule species such as CO adsorbates at binding energies in excess of 1 eV, i.e. even at non-cryogenic temperatures. Future work will explore, whether such

binding configurations can serve as initial states for catalytic activation of CO and other small-molecule species. The facile and conformal nature, in which MoS_2 can be deposited by CVD onto a broad range of oxide substrate suggests great versatility of these findings.

Supporting Information

Energy-Momentum Diagrams showing the dispersion of the single-layer MoS_2 film; Spectroscopic data validating lateral homogeneity of the film; Spectroscopic Data validating the gold deposition thickness; Quantitative comparison of computational CO adsorption energies.

Acknowledgements

We gratefully acknowledge joint funding from DOE grant DE-FG02-07ER15842 (UCF, UCR, UNL). DFT calculations were performed using resource from the National Energy Research Scientific Computing Center (NERSC, project 1996) and the Advanced Research Computing Center at UCF. Synchrotron resources were provided by Elettra. A.E.N as well as C.S.N, S.N.A. and A.G. gratefully acknowledges fellowship support through the National Science Foundation of the United States of America via grants DGE 1326120 and DMR 1359136, respectively.

References

[1] Tuxen, A.; Gobel, H.; Hinnemann, B.; Li, Z. S.; Knudsen, K. G.; Topsoe, H.; Lauritsen, J. V.; Besenbacher, F.; *An atomic-scale investigation of carbon in MoS_2 hydrotreating catalysts sulfided by organosulfur compounds*, *J. Catal.* **2011**, *281*, 345-351.

[2] Surisetty, V. R.; Dalai, A. K.; Kozinski, J.; *Alcohols as alternative fuels: An overview*, *Appl. Catal., A* **2011**, *404*, 1–11.

[3] Saito, M.; Anderson, R. B.; *The activity of Molybdenum compounds for the methanation of CO_2*, *J. Catal.* **1981**, *67*, 296-302.

[4] Osaki, T.; Narita, N.; Horiuchi, T.; Sugiyama, T.; Masuda, H.; Suzuki, K.; *Kinetics of reverse water gas shift (RWGS) reaction on metal disulfide catalysts*, *J. Mol. Catal. A: Chem.* **1997**, *125*, 63-71.

[5] Kim, J.; Byun, S.; Smith, A. J.; Yu, J.; Huang, J. X.; *Enhanced electrocatalytic properties of transition-metal dichalcogenides sheets by spontaneous gold nanoparticle decoration*, *J. Phys. Chem. Lett.* **2013**, *4*, 1227-1232.

[6] Besenbacher, F.; Brorson, M.; Clausen, B. S.; Helveg, S.; Hinnemann, B.; Kibsgaard, J.; Lauritsen, J.; Moses, P. G.; Norskov, J. K.; Topsoe, H.; *Recent STM, DFT and HAADF-STEM studies of sulfide-based hydrotreating catalysts: Insight into mechanistic, structural and particle size effects*, *Catal. Today* **2008**, *130*, 86-96.

[7] Haruta, M.; Yamada, N.; Kobayashi, T.; Iijima, S.; *Gold catalysts prepared by coprecipitation for low-temperature oxidation of hydrogen and of carbon-monoxide*, *J. Catal.* **1989**, *115*, 301-309.

[8] Haruta, M.; Kobayashi, T.; Sano, H.; Yamada, N.; *Novel Gold Catalysts for the Oxidation of Carbon-Monoxide at a Temperature Far Below 0-Degrees-C*, *Chem. Lett.* **1987**, 405-408.

[9] Haruta, A.; *When gold is not noble: Catalysis by nanoparticles*, *Chemical Record* **2003**, *3*, 75-87.

[10] Katsiev, K.; Losovyj, Y.; Lozova, N.; Wang, L.; Mei, W. N.; Zheng, J. X.; Vescovo, E.; Liu, L.; Dowben, P. A.; Goodman, D. W.; *The band structure of carbonmonoxide on 2-D Au islands on graphene*, *Appl. Surf. Sci.* **2014**, *304*, 35-39.

[11] Xu, Y.; Semidey-Flecha, L.; Liu, L.; Zhou, Z. H.; Goodman, D. W.; *Exploring the structure and chemical activity of 2-D gold islands on graphene moire/Ru(0001)*, *Faraday Discuss.* **2011**, *152*, 267-276.

[12] Hammer, B.; Norskov, J. K.; *Why gold Is the noblest of all the metals*, *Nature* **1995**, *376*, 238-240.

[13] Haruta, M.; Tsubota, S.; Kobayashi, T.; Kageyama, H.; Genet, M. J.; Delmon, B.; *Low-temperature oxidation of CO over gold supported on TiO_2, alpha-Fe_2O_3, and Co_3O_4*, *J. Catal.* **1993**, *144*, 175-192.

[14] Chen, M. S.; Goodman, D. W.; *The structure of catalytically active gold on titania*, *Science* **2004**, *306*, 252-255.

[15] Valden, M.; Lai, X.; Goodman, D. W.; *Onset of catalytic activity of gold clusters on titania with the appearance of nonmetallic properties*, *Science* **1998**, *281*, 1647-1650.

[16] Lopez, N.; Janssens, T. V. W.; Clausen, B. S.; Xu, Y.; Mavrikakis, M.; Bligaard, T.; Norskov, J. K.; *On the origin of the catalytic activity of gold nanoparticles for low-temperature CO oxidation*, *J. Catal.* **2004**, *223*, 232-235.

[17] Bondzie, V. A.; Parker, S. C.; Campbell, C. T.; *The kinetics of CO oxidation by adsorbed oxygen on well-defined gold particles on TiO2(110)*, *Catal. Lett.* **1999**, *63*, 143-151.

[18] Cao, W.; Pankratov, V.; Huttula, M.; Shi, X. Y.; Saukko, S.; Huang, Z. J.; Zhang, M.; *Gold nanoparticles on MoS_2 layered crystal flakes*, *Mater. Chem. Phys.* **2015**, *158*, 89-95.

[19] Zhang, P. P.; Lu, X. Y.; Huang, Y.; Deng, J. W.; Zhang, L.; Ding, F.; Su, Z. Q.; Wei, G.; Schmidt, O. G.; *MoS_2 nanosheets decorated with gold nanoparticles for rechargeable Li-O_2 batteries*, *J. Mater. Chem. A* **2015**, *3*, 14562-14566.

[20] Zuo, P.; Jiang, L.; Li, X.; Li, B.; Xu, Y. D.; Shi, X. S.; Ran, P.; Ma, T. B.; Li, D. W.; Qu, L. T.*, et al.*; *Shape-controllable gold nanoparticle MoS_2 hybrids prepared by tuning edge-active sites and surface structures of MoS_2 via temporally shaped femtosecond pulses*, *ACS Appl. Mater. Interfaces* **2017**, *9*, 7447-7455.

[21] Rawal, T. B.; Le, D.; Rahman, T. S.; *Effect of single-layer MoS_2 on the geometry, electronic structure, and reactivity of transition metal nanoparticles*, *J. Phys. Chem. C* **2017**, *121*, 7282-7293.

[22] Janssens, T. V. W.; Carlsson, A.; Puig-Molina, A.; Clausen, B. S.; *Relation between nanoscale Au particle structure and activity for CO oxidation on supported gold catalysts*, *J. Catal.* **2006**, *240*, 108-113.

[23] Visikovskiy, A.; Matsumoto, H.; Mitsuhara, K.; Nakada, T.; Akita, T.; Kido, Y.; *Electronic d-band properties of gold nanoclusters grown on amorphous carbon*, *Phys. Rev. B* **2011**, *83*, 165428.

[24] Koch, H. P.; Laskowski, R.; Blaha, P.; Schwarz, K.; *Adsorption of gold atoms on the h-BN/Rh(111) nanomesh*, *Phys. Rev. B* **2011**, *84*, 245410

[25] Goriachko, A.; He, Y. B.; Over, H.; *Complex growth of NanoAu on BN nanomeshes supported by Ru(0001)*, *J. Phys. Chem. C* **2008**, *112*, 8147-8152.

[26] Ng, M. L.; Preobrajenski, A. B.; Vinogradov, A. S.; Martensson, N.; *Formation and temperature evolution of Au nanoparticles supported on the h-BN nanomesh*, *Surf. Sci.* **2008**, *602*, 1250-1255.

[27] Hansen, L. P.; Ramasse, Q. M.; Kisielowski, C.; Brorson, M.; Johnson, E.; Topsoe, H.; Helveg, S.; *Atomic-scale edge structures on industrial-style MoS_2 nanocatalysts*, *Angew. Chem. Int. Ed. Engl.* **2011**, *50*, 10153-10156.

[28] Mak, K. F.; Lee, C.; Hone, J.; Shan, J.; Heinz, T. F.; *Atomically thin MoS_2: a new direct-gap semiconductor*, *Phys. Rev. Lett.* **2010**, *105*, 136805.

[29] Splendiani, A.; Sun, L.; Zhang, Y. B.; Li, T. S.; Kim, J.; Chim, C. Y.; Galli, G.; Wang, F.; *Emerging photoluminescence in monolayer MoS_2 Nano Lett.* **2010**, *10*, 1271-1275.

[30] Jin, W. C.; Yeh, P. C.; Zaki, N.; Zhang, D. T.; Sadowski, J. T.; Al-Mahboob, A.; van der Zande, A. M.; Chenet, D. A.; Dadap, J. I.; Herman, I. P.*, et al.*; *Direct measurement of the thickness-dependent electronic band structure of MoS_2 using angle-resolved photoemission spectroscopy*, *Phys. Rev. Lett.* **2013**, *111*, 041407.

[31] Miwa, J. A.; Ulstrup, S.; Sorensen, S. G.; Dendzik, M.; Cabo, A. G.; Bianchi, M.; Lauritsen, J. V.; Hofmann, P.; *Electronic structure of epitaxial single-layer MoS_2*, *Phys. Rev. Lett.* **2015**, *114*, 046802.

[32] Kormanyos, A.; Burkard, G.; Gmitra, M.; Fabian, J.; Zolyomi, V.; Drummond, N. D.; Fal'ko, V.; *k.p theory for two-dimensional transition metal dichalcogenide semiconductors*, *2D Mat.* **2015**, *2*, 022001.

[33] Latzke, D. W.; Zhang, W. T.; Suslu, A.; Chang, T. R.; Lin, H.; Jeng, H. T.; Tongay, S.; Wu, J. Q.; Bansil, A.; Lanzara, A.; *Electronic structure, spin-orbit coupling, and interlayer interaction in bulk MoS_2 and WS_2*, *Phys. Rev. B* **2015**, *91*, 235202

[34] Mann, J.; Sun, D.; Ma, Q.; Preciado, E.; Yamaguchi, K.; Chen, J.-R.; Heinz, T. F.; Kawakami, R.; Bartels, L.; *Facile growth of sub-millimeter scale monolayer MoS_2 films on SiO_2/Si*, *Eur. Phys. J. B* **2013**, *86*, 226.

[35] Plechinger, G.; Mann, J.; Preciado, E.; Barroso, D.; Nguyen, A.; Eroms, J.; Schuller, C.; Bartels, L.; Korn, T.; *A direct comparison of CVD-grown and exfoliated MoS_2 using optical spectroscopy*, *Semicond. Sci. Technol.* **2014**, *29*, 064008.

[36] Ma, Q.; Odenthal, P. M.; Mann, J.; Le, D.; Wang, C. S.; Zhu, Y. M.; Chen, T. Y.; Sun, D. Z.; Yamaguchi, K.; Tran, T.*, et al.*; *Controlled argon beam-induced desulfurization of monolayer molybdenum disulfide*, *J. Phys.-Condens. Mat.* **2013**, *25*, 252201.

[37] Ma, Q.; Isarraraz, M.; wang, C.; Preciado, E.; Klee, V.; Bobek, S.; Yamaguchi, K.; li, E.; Odenthal, P. M.; nguyen, A.*, et al.*; *Postgrowth tuning of the bandgap of single-layer molybdenum disulfide films by sulfur/selenium exchange*, *ACS Nano* **2014**, *8*, 4672-4677.

[38] Kresse, G.; Joubert, D.; *From ultrasoft pseudopotentials to the projector augmented-wave method*, *Phys. Rev. B* **1999**, *59*, 1758–1775.

[39] Blöchl, P. E.; *Projector augmented-wave method*, *Phys. Rev. B* **1994**, *50*, 17953–17979.

[40] Perdew, J. P.; Burke, K.; Ernzerhof, M.; *Generalized gradient approximation made simple*, *Phys. Rev. Lett.* **1996**, *77*, 3865-3868.

[41] Grimme, S.; Antony, J.; Ehrlich, S.; Krieg, H.; *A consistent and accurate ab initio parametrization of density functional dispersion correction (DFT-D) for the 94 elements H-Pu*, *J. Chem. Phys.* **2010**, *132*, 154104.

[42] Man, M. K. L.; Deckoff-Jones, S.; Winchester, A.; Shi, G. S.; Gupta, G.; Mohite, A. D.; Kar, S.; Kioupakis, E.; Talapatra, S.; Dani, K. M.; *Protecting the properties of monolayer MoS_2 on silicon based substrates with an atomically thin buffer*, *Sci. Rep.* **2016**, *6*, 20890

[43] Su, S.; Zhang, C.; Yuwen, L. H.; Chao, J.; Zuo, X. L.; Liu, X. F.; Song, C. Y.; Fan, C. H.; Wang, L. H.; *Creating SERS hot spots on MoS_2 nanosheets with in situ grown gold nanoparticles*, *ACS Appl. Mater. Interfaces* **2014**, *6*, 18735-18741.

[44] Kwon, K. C.; Choi, S.; Hong, K.; Moon, C. W.; Shim, Y. S.; Kim, D. H.; Kim, T.; Sohn, W.; Jeon, J. M.; Lee, C. H.*, et al.*; *Wafer-scale transferable molybdenum disulfide thin-film catalysts for photoelectrochemical hydrogen production*, *Energ Environ Sci* **2016**, *9*, 2240-2248.

[45] Chernikov, A.; Berkelbach, T. C.; Hill, H. M.; Rigosi, A.; Li, Y. L.; Aslan, O. B.; Reichman, D. R.; Hybertsen, M. S.; Heinz, T. F.; *Exciton binding energy and nonhydrogenic Rydberg series in monolayer WS_2*, *Phys. Rev. Lett.* **2014**, *113*, 076802.

[46] He, K. L.; Kumar, N.; Zhao, L.; Wang, Z. F.; Mak, K. F.; Zhao, H.; Shan, J.; *Tightly bound excitons in monolayer WSe_2*, *Phys. Rev. Lett.* **2014**, *113*, 026803

[47] Lin, Y. X.; Ling, X.; Yu, L. L.; Huang, S. X.; Hsu, A. L.; Lee, Y. H.; Kong, J.; Dressehaus, M. S.; Palacios, T.; *Dielectric screening of excitons and trions in single-layer MoS_2*, *Nano Lett.* **2014**, *14*, 5569-5576.

[48] Prescott Evens; Takat B. Rawal; Sahar Naghibi Alvillar; Yaroslav Lasovyj; Khabiboulakh Katsiev; Ludwig Bartels; Talat S. Rahman; Peter A. Dowben; Jeong, H.-K., *To be published* **2017**.

[49] Fukutani, K.; Hayashi, H.; Yakovkin, I. N.; Habuchi, T.; Hirayama, D.; Jiang, J.; Iwasawa, H.; Shimada, K.; Losovyj, Y. B.; Dowben, P. A.; *Enhanced electron-phonon coupling at the Au/Mo(112) surface*, *Phys. Rev. B* **2012**, *86*, 205432

[50] Zhou, Y. Y.; Lawrence, N. J.; Wang, L.; Kong, L. M.; Wu, T. S.; Liu, J.; Gao, Y.; Brewer, J. R.; Lawrence, V. K.; Sabirianov, R. F.*, et al.*; *Resonant Photoemission Observations and DFT Study of s-d Hybridization in Catalytically Active Gold Clusters on Ceria Nanorods*, *Angew. Chem. Int. Ed. Engl.* **2013**, *52*, 6936-6939.

[51] Neumaier, M.; Weigend, F.; Hampe, O.; Kappes, M. M.; *Binding energy and preferred adsorption sites of CO on gold and silver-gold cluster cations: Adsorption kinetics and quantum chemical calculations*, *Faraday Discuss.* **2008**, *138*, 393-406.

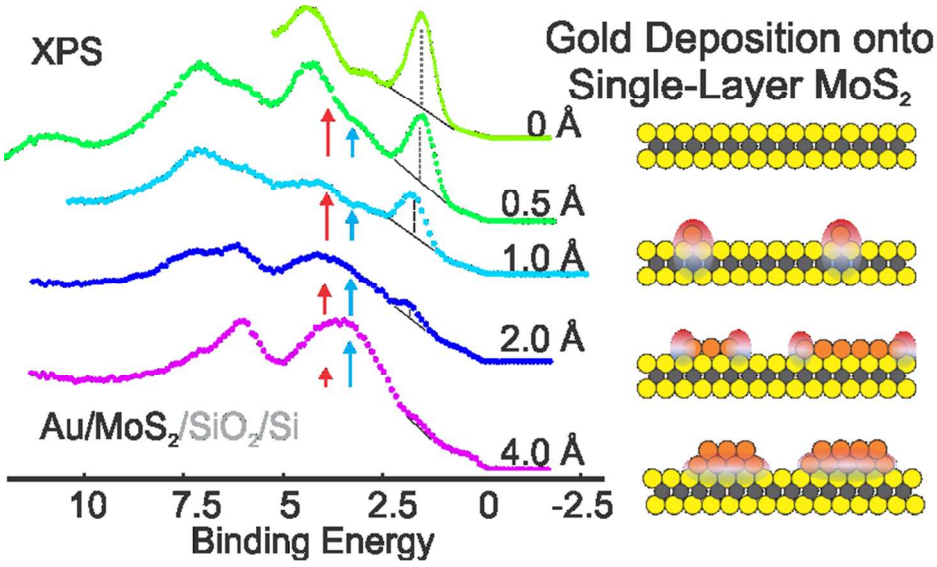

Table of Contents Grpahics

76x42mm (300 x 300 DPI)